Organic & Biomolecular Chemistry

Accepted Manuscript

ROYAL SOCIETY OF CHEMISTRY

www.rsc.org/obc

Organic & Biomolecular Chemistry RSCPublishing

Paper

Facile and High-yield Formation of Dipyrrin-Boronic Acid Dyads and Triads: Light-Harvesting System in the Visible Region Based on Efficient Energy Transfer

Cite this: DOI: 10.1039/xoxxoooooox

Received ooth January 2012,
Accepted ooth January 2012

DOI: 10.1039/xoxxoooooox

www.rsc.org/

Masaki Yamamura,[a] Shinya Yazaki,[a] Motofumi Seki,[a] Yasunori Matsui,[b] Hiroshi Ikeda,[b] Tatsuya Nabeshima*[a]

Artificial light-harvesting systems, *Ar*,*O*-BODIPY dyads and triads conjugated with a light harvester, were synthesized in high yield by the reaction of an N2O2-type dipyrrin with boronic acids. Dyad **2** having a pyrene unit underwent quantitative Förster-type resonance energy transfer (FRET) from the antenna unit, pyrene, to the fluorophore unit, *Ar,O*-BODIPY. Triads **3**·**5** and **4**·**5** were quantitatively prepared by mixing pyridine-appended compounds **3** and **4** with saloph·Zn complex **5**, respectively. Triad **4**·**5** underwent efficient FRET from the saloph·Zn complex unit to the fluorophore unit at the rate of 2.0×10^{11} s^{-1}. Interestingly, the fluorescence quenching process in the excited state of the triad **3**·**5** took place following the energy transfer event. Thus, appropriate positioning of the energy donor and acceptor is necessary to construct a highly efficient FRET system.

Introduction

Energy and electron transfer in a photoexcited state is an important phenomenon in nature. In photosynthesis of plants, energy transfer between chlorophylls, light-harvesting pigments, plays a crucial role in collecting photon energy.[1] A variety of artificial light-harvesting systems inspired by the natural system have been developed.[2]

Borondipyrromethenes (BODIPYs) are interesting chromophores featuring intense absorption and fluorescence and excellent stability against light and chemicals.[3] Thus, BODIPYs are applicable to chemosensors, biolabels, organic light-emitting diodes, etc. The conjugation of BODIPYs with energy or electron donor units has led to the realization of BODIPY light harvesting systems,[4] which are applicable to molecular probes,[5] photo-caged compounds,[6] and dye-sensitized solar cells.[7] In the BODIPY conjugates, the connection of the donor subunits to a central boron atom ensures good electronic communication.[8] However, the synthetic methods for the BODIPYs connected with the donor subunits on the boron have been usually limited to nucleophilic substitution with a strong base such as an organometallic compound, Grignard, or organolithium reagents. These methods resulted in low or moderate yields of products and complicated purification in many cases. Recently, the complexation of dipyrrin, which is an organic ligand unit of BODIPY, has provided energy-transfer systems via dipyrrin-Zn complex units.[9] However, these systems suffered from low synthetic yields (2~3%) due to non-selective connection. We reported a synthetic strategy for the preparation of BODIPYs having various substituents on the boron center by reaction of an N_2O_2-type tetradentate dipyrrin ligand with boronic acids.[10] This reaction has significant advantages: no additives or catalyst, high-yield synthesis, and reversible formation that makes the functional group on the boron exchangeable.[11] The last one is useful in designing supramolecular architectures because the reversible dynamic bond is necessary for the facile construction of supramolecular structures. Additionally, complexes of the N_2O_2-type dipyrrin feature strong fluorescence in the red-to-near infrared (NIR) region, which is redshifted compared to basic BODIPYs.[12] Thus, the N_2O_2-type dipyrrin complexes can be applicable to a light-harvesting system that absorbs visible light over a broad range to emit light in the deep red region.

Here, BODIPYs conjugated with a light harvester are synthesized by forming dyads of an N_2O_2-type dipyrrin and a boronic acid, "*Ar*,*O*-BODIPYs" and triads of a metal complex and *Ar*,*O*-BODIPY having a coordination site (Figure 1). In the *Ar*,*O*-BODIPY dyad and triad, the *Ar*-group was equipped as an energy donor unit. The facile energy donor−acceptor system exhibited highly efficient (nearly quantitative) energy transfer from the excited donor unit.

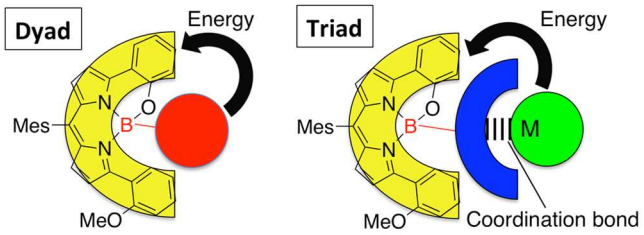

Figure 1. Photoinduced energy transfer from donor to acceptor in *Ar*,*O*-BODIPY dyad and triad.

Experimental

General remarks

All reactions were performed under a dry nitrogen atmosphere. Organic solvents were purchased as pre-dried solvents and used without any further purification. Starting materials **1**,[13] pyrenylboronic acid,[14] pyridylboronic acid,[15] and **5**[16] were synthesized according to the literature method. ^{1}H and ^{13}C NMR spectra were recorded by a Bruker AVANCE400 using TMS as an internal reference. High-resolution ESI-TOF mass spectra were recorded by an Applied Biosystems TripleTOF4600. ESI-TOF mass spectra of complexes were recorded by a JEOL JMS-T100CS. MALDI-TOF mass spectra were recorded by an AB Sciex TOF/TOF5800. Melting points were obtained using a Yanaco melting point apparatus and are uncorrected.

Synthesis of 2

A toluene/methanol solution (5 mL/1 mL) of **1** (9.8 mg, 21.3 μmol) and 1-pyrenylboronic acid (8.2 mg, 33 μmol) was refluxed for 40 hours. After evaporation of solvent, the residual product was purified by silica-gel column chromatography (eluent: chloroform/hexane) to give purple powder of **2** (13.2 mg, 92%). **2**: purple powder, ^{1}H NMR (400 MHz, $CDCl_3$) δ 8.23 (d, *J* = 9.2 Hz, 1H), 7.98-7.95 (m, 3H), 7.89-7.81 (m, 3H), 7.68 (d, *J* = 8.0 Hz, 1H), 7.63 (d, *J* = 8.0 Hz, 1H), 7.53 (td, *J* = 8.0 Hz, 1.5 Hz, 1H), 7.46 (d, *J* = 9.2 Hz, 1H), 7.35 (dd, *J* = 8.0 Hz, 1.5 Hz, 1H), 7.22-7.18 (m, 2H), 7.12 (dd, *J* = 8.0 Hz, 1.0 Hz, 1H), 7.08 (s, 1H), 7.02 (s, 1H), 6.90 (d, *J* = 4.4 Hz, 1H), 6.76 (d, *J* = 4.4 Hz, 1H), 6.71 (td, *J* = 8.0 Hz, 1.0 Hz, 1H), 6.63 (d, *J* = 8.0 Hz, 1H), 6.62 (d, *J* = 4.4 Hz, 1H), 6.31 (d, *J* = 4.4 Hz, 1H), 2.62 (s, 3H), 2.57 (s, 3H), 2.42 (s, 3H), 2.19 (s, 3H); ^{13}C{^{1}H} NMR (150 MHz, $CDCl_3$) δ 158.27 (*C*H), 156.03 (*C*H), 155.91 (*C*H), 149.91 (*C*H), 142.38 (*C*H), 138.48 (*C*H), 137.17 (*C*H), 137.08 (*C*H), 136.82 (*C*H), 133.97 (*C*H), 133.80 (*C*H), 133.50 (*C*H), 132.70 (*C*H), 131.61 (*C*H), 131.32 (*C*H), 130.99 (*C*H), 130.69 (*C*H), 130.01 (*C*H), 128.47 (*C*H), 128.39 (*C*H), 128.35 (*C*H), 127.70 (*C*H), 127.52 (*C*H), 127.49 (*C*H), 126.23 (*C*H), 125.74 (*C*H), 124.95 (*C*H), 124.88 (*C*H), 124.84 (*C*H), 124.39 (*C*H), 123.61 (*C*H), 123.56 (*C*H), 122.03 (*C*H), 121.26 (*C*H), 119.98 (*C*), 119.74 (*C*H), 119.22 (*C*), 119.07 (*C*), 115.37 (*C*), 111.18 (*C*), 54.85 (CH_3), 21.24 (CH_3), 21.01 (CH_3), 20.24 (CH_3); HR-MS (ESI-TOF) $C_{47}H_{35}BN_2O_2Na$ $[M+Na]^+$ calcd *m*/*z* 693.2689, found *m*/*z* 693.2686.

Synthesis of 3

To a toluene solution (10 mL) of **1** (28.5 mg, 61.9 μmol) was added a methanol solution (4 mL) of 3-pyridylboronic acid (58.0 mg, 0.47 mmol). The mixture was refluxed for 15 hours. After evaporation of solvent, the residual product was purified by silica-gel column chromatography (eluent: chloroform/ethyl acetate) to give purple powder of **3** (33.4 mg, 99%). **3**: purple powder, mp > 270 °C; ^{1}H NMR (600 MHz, $CDCl_3$) δ 8.16 (dd, *J* = 4.5 Hz, 1.5 Hz, 1H), 7.97 (s, 1H), 7.70 (dd, *J* = 7.5 Hz, 1.5 Hz, 1H), 7.48 (dd, *J* = 7.5 Hz, 4.5 Hz, 1H), 7.42 (dd, *J* = 7.8 Hz, 1.5 Hz, 1H), 7.24 (td, *J* = 7.8 Hz, 1.5 Hz, 1H), 7.09 (t, *J* = 7.8 Hz, 1H), 7.01 (s, 1H), 7.00 (d, *J* = 7.8 Hz, 1H), 6.98 (s, 1H), 6.91 (d, *J* = 7.8 Hz, 1H), 6.89 (d, *J* = 7.8 Hz, 1H), 6.82 (d, *J* = 7.8 Hz, 1H), 6.79 (d, *J* = 7.8 Hz, 1H), 6.78 (d, *J* = 4.4 Hz, 1H), 6.72 (d, *J* = 4.4 Hz, 1H), 6.67 (d, *J* = 4.4 Hz, 1H), 6.48 (d, *J* = 4.4 Hz, 1H), 3.49 (s, 3H), 2.39 (s, 3H), 2.34 (s, 3H), 2.15 (s, 3H); ^{13}C{^{1}H} NMR (150 MHz, $CDCl_3$) δ 157.83 (*C*H), 156.33 (*C*H), 154.93 (*C*H), 152.50 (*C*H), 149.39 (*C*H), 147.24 (*C*H), 142.38 (*C*H), 138.86 (*C*H), 138.48 (*C*H), 136.96 (*C*H), 136.74 (*C*H), 136.41 (*C*H), 133.16 (*C*H), 133.08 (*C*H), 132.84 (*C*H), 131.01 (*C*H), 130.30 (*C*H), 128.27 (*C*H), 128.25 (*C*H), 127.97 (*C*H), 127.33 (*C*H), 125.83 (*C*H), 122.22 (*C*H), 121.81 (*C*H), 121.07 (*C*H), 119.94 (*C*), 119.66 (*C*H), 118.96 (*C*), 118.40 (*C*), 114.96 (*C*), 110.56 (*C*), 55.49 (CH_3), 21.19 (CH_3), 20.55 (CH_3), 20.11 (CH_3); HR-MS (ESI-TOF) $C_{36}H_{31}BN_3O_2$ $[M+H]^+$ calcd *m*/*z* 548.2509, found *m*/*z* 548.2512; Anal. Calcd for $C_{36}H_{30}BN_3O_2 \cdot 0.5H_2O$: C, 77.70; H, 5.62; N, 7.55. Found: C, 77.79; H, 5.65; N, 7.50.

Synthesis of 4

A toluene solution (10 mL) of **1** (30.8 mg, 66.9 μmol) and 4-pyridylboronic acid (18.6 mg, 0.151 mmol) was refluxed for 14 hours. To this were added methanol (3 mL) and further boronic acid (13.0 mg, 0.106 mmol) and then the mixture was refluxed for 12 hours. After evaporation of solvent, the residual product was purified by silica-gel column chromatography (eluent: dichloromethane/ethyl acetate) to give purple powder of **4** (35.3 mg, 96%). **4**: purple powder, mp > 270 °C; ^{1}H NMR (600 MHz, $CDCl_3$) δ 8.09 (dd, *J* = 4.8 Hz, 1.5 Hz, 2H), 7.71 (dd, *J* = 7.8 Hz, 1.5 Hz, 1H), 7.49-7.43 (m, 2H), 7.27 (td, *J* = 7.8 Hz, 1.5 Hz, 1H), 7.09 (t, *J* = 7.8 Hz, 1H), 7.08 (td, *J* = 7.8 Hz, 1.0 Hz, 1H), 7.02 (s, 1H), 6.90 (s, 1H), 6.91 (dd, *J* = 7.8 Hz, 1.0 Hz, 1H), 6.88 (d, *J* = 7.8 Hz, 1H), 6.83 (td, *J* = 7.8 Hz, 1.0 Hz, 1H), 6.77 (d, *J* = 4.4 Hz, 1H), 6.73 (d, *J* = 4.4 Hz, 1H), 6.68 (d, *J* = 4.4 Hz, 1H), 6.65 (d, *J* = 4.8 Hz, 2H), 6.49 (d, *J* = 4.4 Hz, 1H), 3.50 (s, 3H), 2.39 (s, 3H), 2.32 (s, 3H), 2.15 (s, 3H); ^{13}C{^{1}H} NMR (150 MHz, $CDCl_3$) δ 157.98 (*C*), 156.40 (*C*), 155.13 (*C*), 149.42 (*C*), 147.92 (*C*H), 142.55 (*C*), 138.65 (*C*), 136.98 (*C*), 136.84 (*C*), 136.65 (*C*), 133.23 (*C*H), 133.17 (*C*H), 132.96 (*C*H), 131.12 (*C*H), 130.33 (*C*), 128.39 (*C*H), 128.12 (*C*H), 127.52 (*C*H), 126.52 (*C*H), 125.95 (*C*H), 121.83 (*C*), 121.29 (*C*H), 119.97 (*C*H), 119.82 (*C*H), 119.06 (*C*H), 118.37 (*C*), 115.01 (*C*H), 110.56 (*C*H), 55.51 (CH_3), 21.29 (CH_3), 20.57 (CH_3), 20.19 (CH_3); HR-MS (ESI-TOF) $C_{36}H_{31}BN_3O_2$ $[M+H]^+$ calcd *m*/*z* 548.2509, found *m*/*z* 548.2512; Anal. Calcd for $C_{36}H_{30}BN_3O_2 \cdot 0.4H_2O$: C, 77.96; H, 5.60; N, 7.58. Found: C, 78.01; H, 5.66; N, 7.35.

Electrochemical Studies

The cyclic voltammograms (CV) were recorded using a BAS ALS/CHI model 750A. An $Ag/AgNO_3$ reference electrode was used. The working electrode was a 1-mm-diameter glassy carbon with a platinum wire acting as the counter electrode. The CV was taken at a scan rate of 100 mV/s. After CV measurements in 0.1 M Bu_4NClO_4/CH_2Cl_2 without any internal reference, ferrocene was added to the same sample and the electrochemical potential was adjusted to ferrocenium/ferrocene as the internal reference (Fc/Fc^+ = 0.20 V).

Photophysical Studies

UV−vis absorption spectra were recorded on a JASCO Ubest V-660. Fluorescence spectra were recorded on a JASCO FP-8600. Absolute fluorescence quantum yields (Φ_{flu}) were measured using a Hamamatsu Photonics absolute PL quantum yield measurement system C9920-02.[17] Fluorescence decay measurements were performed using a Horiba Jobin Yvon FluoroCube. Sample solutions were excited by a diode laser at 371 nm before and after an argon gaseous bubbling for three minutes. Transient absorption spectra were recorded using a suite of Unisoku TSP-1000 with a 150 W Xe lamp and a Spectra Physics Quanta-Ray GC-100 (fwhm = 8 ns) Nd:YAG pulsed laser (355 nm). Sample solutions were degassed via five freeze (77 K)−pump (0.1 mmHg)−thaw (ambient temperature) cycles prior to the measurement.

Computational Methods

The DFT calculations were performed using the Gaussian09 packages[18] with the M06-2X functional.[19] The geometry optimizations were performed using the basis set 6-31G(d,p). Time-dependent calculations were performed at the equilibrium geometries using the basis set 6-31G(d,p).

Results and discussion

The tridentate dipyrrin ligand **1**, one OH group of which was protected by a Me group, was synthesized by the previously-reported procedure.[13] The reaction of **1** with boronic acid gave the dyads of dipyrrin and boronic acid in high yields, *Ar*,*O*-BODIPYs **2** (92%), **3** (99%), and **4** (96%) (Scheme 1).

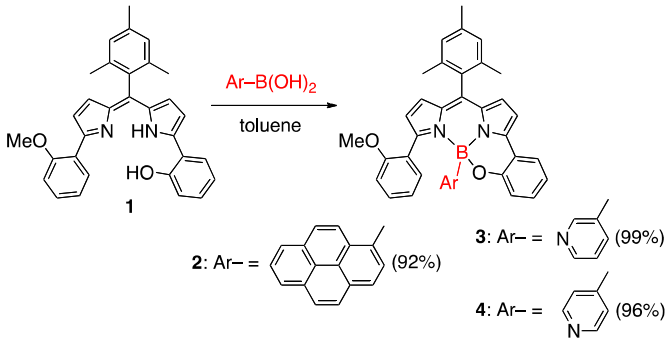

Scheme 1.

The absorption spectra of *Ar*,*O*-BODIPY **2**−**4** have almost the same maximum at 595 nm with a large molar absorption coefficient (~4 × 10^4 $cm^{-1}·M^{-1}$), assigned to the S_0−S_1 transition of BODIPY (Figure 2). Only in **2**, higher energy absorptions were observed between 350~450 nm, which are assigned to π,π* transitions of the pyrene unit (Figure 2). The absorption spectrum of **2** was almost a simple combination of those of the BODIPY and pyrene units. This implies no electronic coupling between the BODIPY and pyrene units on the boron centre in the ground state. Fluorescence spectra of **2**, **3**, and **4** exhibit emission bands with maxima at 650, 642, and 643 nm, respectively (Figure 2), which are similar to those of reported *Ar*,*O*-BODIPYs (642−644 nm).[10] The Φ_{flu} values of **2**, **3**, and **4** were determined by an integrating sphere method to be high values, 56, 56, and 59%, respectively (Table 1), which are also comparable to those of reported *Ar*,*O*-BODIPYs (59~62%).[10]

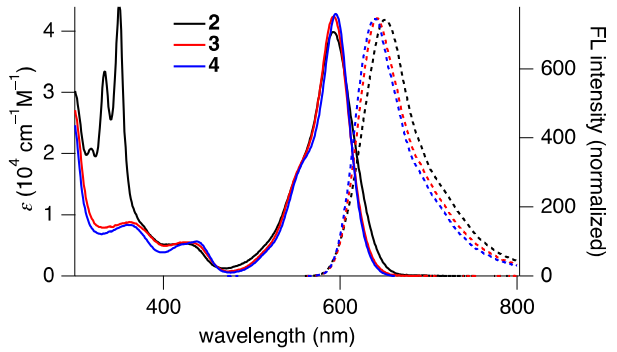

Figure 2. UV−vis absorption (lines) and fluorescence spectra (dots, λ_{ex} = 550 nm) of **2** (black), **3** (red), and **4** (blue) in chloroform (5.0×10^{-6} M).

The excitation spectrum of **2** collected at 650 nm fits well with the absorption spectrum (Figure 3a). In the fluorescence-excitation 3D spectrum, no fluorescence based on the pyrene unit was observed (Figure 3b). The excitation spectra well fit the absorption spectra regardless of the fluorescence wavelengths. The Φ_{flu} value obtained by 350-nm excitation, 55%, is almost the same as that obtained by 550-nm excitation, 56%. These results strongly indicate quantitative energy transfer from the antenna unit, pyrene, to the fluorophore unit, *Ar*,*O*-BODIPY. The lifetime of excited pyrene is so long (~400 ns) that efficient energy transfer can take place before nonradiative deactivation.

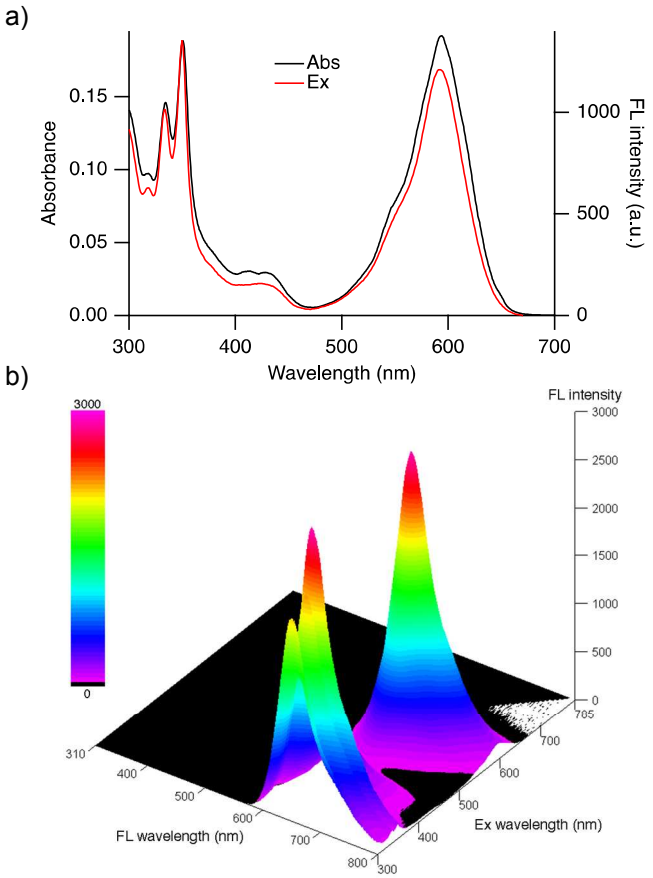

Figure 3. (a) Absorption and excitation spectra (λ_{flu} = 650 nm) and (b) 3D fluorescence versus excitation spectrum of **2** in chloroform. [**2**] = 5×10^{-6} M.

Table 1. Optical Properties and Photophysical Data[a]

	λ_{abs} (nm)	λ_{flu} (nm)[b]	E^{0-0} (eV)[c]	Φ_{flu}[b]	τ_{flu} (ns)	k_r (10^7 s^{-1})[d]	k_{nr} (10^7 s^{-1})[e]
2	350, 370, 595	650	2.00	0.56	9.0	6.2	4.9
3	595	642	2.01	0.56	9.1	6.2	4.8
3·**5**	429, 599	644	2.00	0.066	4.6 (37%), 8.9 (62%)	0.53, 0.46	12.9
4	595	643	2.01	0.59	9.1	6.5	4.5
4·**5**	430, 595	644	2.00	0.55	9.4	5.9	4.8
5	412	550	2.63	0.027	0.5	5.4	194.6

[a] [**2**] = 5.0 × 10^{-6} M in dichloromethane and [**3**] = [**4**] = [**5**] = 1.0 × 10^{-5} M in *n*-hexane. [b] Excited at 595, 595, 599, 595, 595 and 412 nm for **2**, **3**, **3**·**5**, **4**, **4**·**5**, and **5**. [c] $E^{0-0} = (1240/\lambda_{abs} + 1240/\lambda_{flu})/2$. [d] $k_r = \Phi_{flu}/\tau_{flu}$. [e] $k_{nr} = (1 - \Phi_{flu})/\tau_{flu}$.

Next, a triad system was prepared by conjugation of the dyad *Ar*,*O*-BODIPY **3** and **4** with saloph·Zn complex **5** (Chart 1).[20] *Ar*,*O*-BODIPY **3** and **4** were nearly transparent around 470 nm (Figure 4a). Conversely, **5** shows intense absorption at the transparent region of **3** and **4**. The ε value of **5** at 470 nm (13000 $cm^{-1}\cdot M^{-1}$) is more than 16 times as large as those of **3** and **4** (800 $cm^{-1}\cdot M^{-1}$). Furthermore, fluorescence of **5** with the maximum at 550 nm overlaps the absorption of **3** and **4**. Thus, **5** is expected to absorb the photon in the nearly transparent region of **3** and **4**, and then transfer its excitation energy to *Ar*,*O*-BODIPY via Förster-type resonance energy transfer (FRET) mechanism.

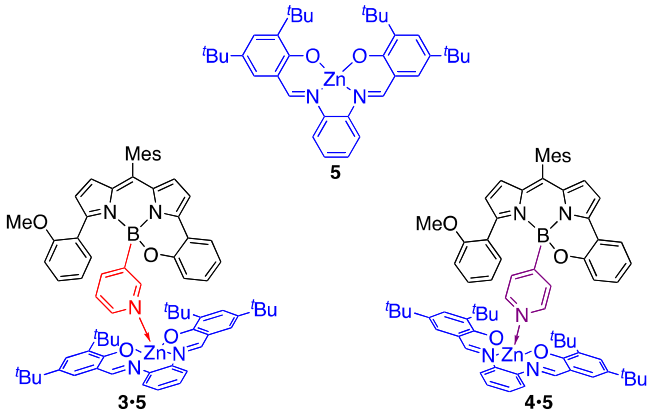

Chart 1.

To clarify the triad formation, spectroscopic titrations were performed in *n*-hexane. A slight bathochromic shift of the absorption maximum of **3** was observed upon the addition of **5** (Figure 4a). This shift was nearly saturated by the addition of one equivalent of **5** (Figure 4b). This result suggests the formation of a 1:1 adduct **3**·**5**. The presence of isosbestic points also supports that only one product coexists at the equilibrium point. The association constant was calculated to be (7.3 ± 2.3) × 10^7 M^{-1}. The estimated formation ratio of adduct **3**·**5** is 96% at the concentration of 5.0 × 10^{-6} M. All the spectral and photophysical measurements of the triads were performed at a concentration of 5.0 × 10^{-6} M, at which the dissociation process of the triads in the ground state is negligible. In spectroscopic titration of **4** with **5**, the spectral change was too small to determine the association constant (Figure S19). However, the isosbestic points indicate the formation of **4**·**5**.

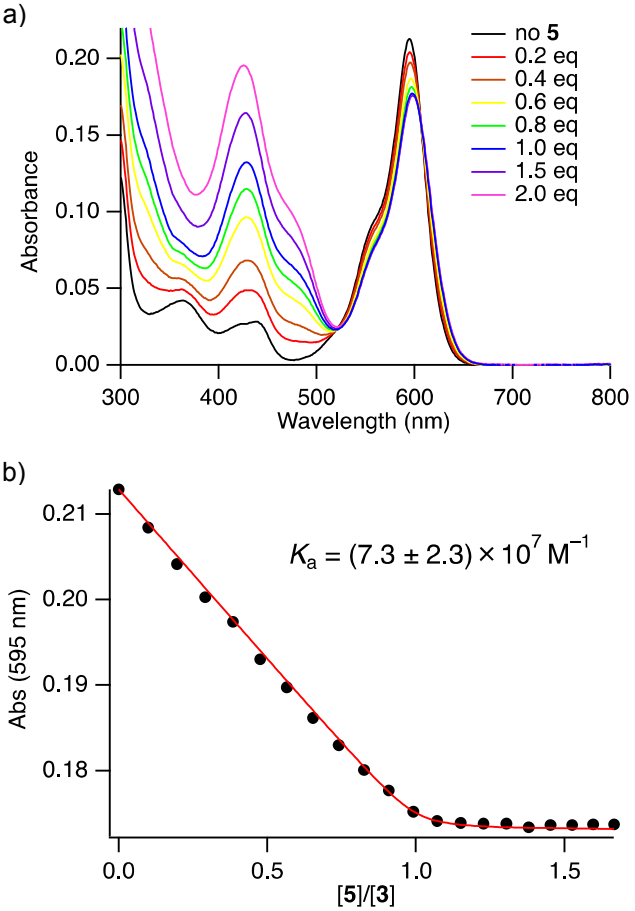

Figure 4. (a) UV−vis spectroscopic titration of **3** with the addition of **5** (*n*-hexane, [**3**] = 5.0 × 10^{-6} M). (b) Plot of absorbance at 595 nm vs [**5**]/[**3**] and calculated binding isotherm.

The ESI mass spectrum also confirmed the formation of **3**·**5** by the observation of a peak at *m*/*z* = 1150.53 corresponding to [**3**·**5**+H]$^+$ (Figure S7 and S8). In the ^{1}H NMR spectrum of **3**·**5**, the two protons (*b* and *b'*) of the imine moieties of **5** appeared nonequivalently due to the chiral boron centre (Figure 5). This indicates that the Zn–pyridine bond is sufficiently inert on the NMR timescale.

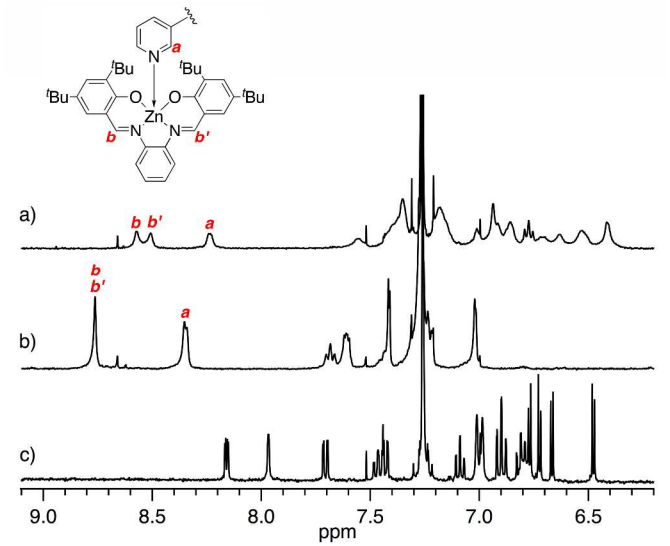

Figure 5. ^{1}H NMR spectra of (a) **3**·**5**, (b) **5**·pyridine, and (c) **3** ($CDCl_3$, 1.0×10^{-3} M).

The fluorescence spectrum of **3**·**5** exhibits one emission band based on *Ar*,*O*-BODIPY (640 nm) without **5**-based emission (550 nm) even when excited at 470 nm (Figure 6a). The excitation spectrum of **3**·**5** is similar to the absorption spectrum (Figure S12). These results indicate FRET from **5** to **3**. However, Φ_{flu} of **3**·**5** (6.6%) was much smaller than that of **3** (56%). The fluorescence intensity of **3**·**5** was more than 2.2 times as large as that of **3** upon excitation at 470 nm. This difference in fluorescence intensity is consistent with the Φ_{flu} and ε values.

In contrast to **3**, the fluorescence of **4** drastically increased upon addition of **5** (Figure 6b). The Φ_{flu} value of **4**·**5** (55%) is as high as that of **4** (59%) because the fluorescence of **4**·**5** is not quenched. When excited at 470 nm, the fluorescence intensity of **4**·**5** is 17 times as large as that of **4** due to the enhancement of the absorbance. Noteworthy is that the small difference in **3**·**5** and **4**·**5**, regioisomers at the pyridine-position, can drastically affect the Φ_{flu}. The colour of an *n*-hexane solution of **3**·**5** was distinctly different from that of **4**·**5** reflecting the difference in their Φ_{flu} (Figure 6, insets). Colour of **3** changed from red to green upon the addition of **5**, while the red fluorescent colour of **4** was maintained after the addition of **5**.

Efficiency of FRET in **4**·**5** was estimated to be 99% by considering the quantum yields 54.8% and 55.3%, obtained by 420- and 600-nm excitations, respectively (Figure 7). The excitation spectrum of **4**·**5** is almost the same as the absorption spectrum, which also indicates the nearly quantitative FRET from the **5** unit to the *Ar*,*O*-BODIPY unit (Figure S13). Although **5*** deactivates rapidly with a rate of 2.0×10^9 s^{-1}, FRET took place much more rapidly. The rate constant of the FRET was estimated to be 2.0×10^{11} s^{-1}, which indicates a highly efficient process.

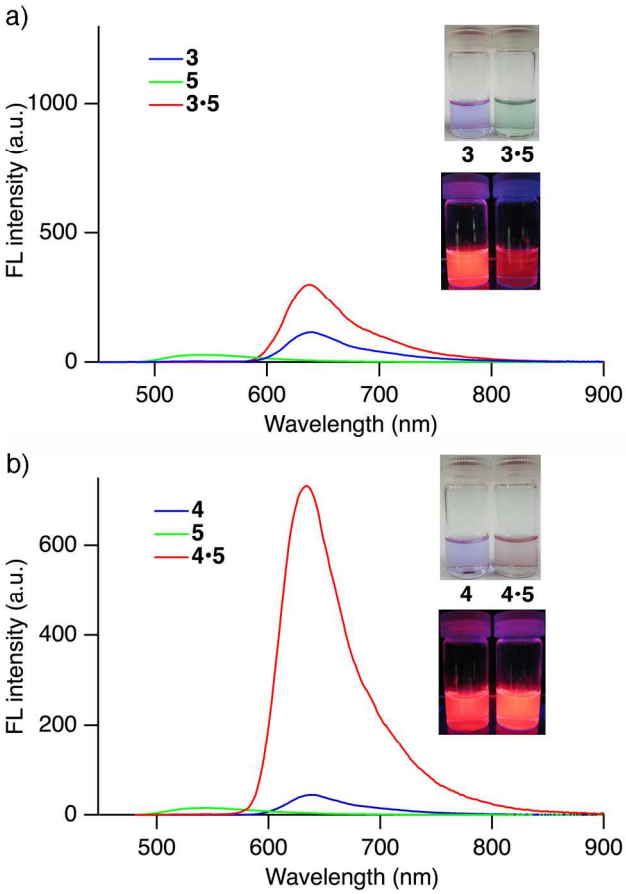

Figure 6. Fluorescence spectra of (a) **3**, **5**, and **3**·**5** and (b) **4**, **5**, and **4**·**5** (*n*-hexane, 5.0×10^{-6} M, λ_{ex} = 470 nm). Insets show the photography of **3** and **4** before and after addition of **5**.

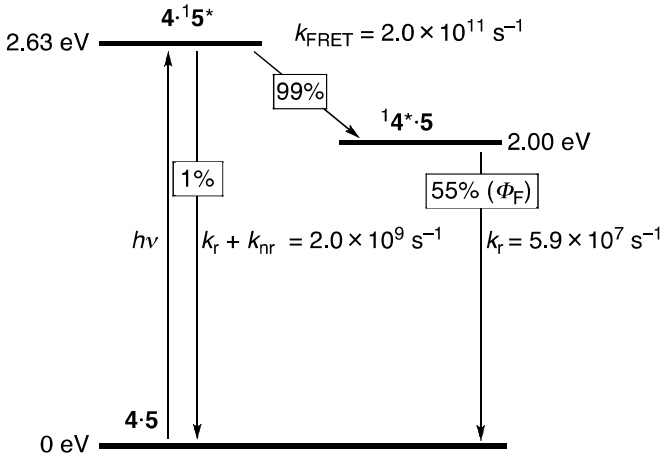

Figure 7. An energy diagram for a FRET pathway of **4**·**5**. The energy values are relative to that of the ground state of **4**·**5**.

The triad **3**·**5** exhibited weak fluorescence in contrast to **4**·**5**. Even when the BODIPY core of **3**·**5** was directly excited by 600-nm light, Φ_{flu} was largely lowered (6.6%), which indicates the fluorescence quenching of the BODIPY core by **5**.[21] One possible pathway for the quenching is exciplex $(\mathbf{3}^{\delta-}\cdot\mathbf{5}^{\delta+})$* formation[22] by charge transfer interaction between **3*** and **5** (Figure 8). In CV measurements, the high reduction potential, E_{red}, of acceptor **3** and a low oxidation potential, E_{ox}, of donor **5**·pyridine were determined to be –1.21 V and +0.55 V,

respectively (vs Fc/Fc^+ = +0.20 V, Figures S9–S11). In addition, the DFT calculation also affords a low LUMO level of **3** (–1.98 eV) and a high HOMO level of **5**·pyridine (–6.07 eV) at the M06-2X/6-31(d,p) level (Figure 9). The calculated singlet-excitation energies of **3** and **5**·pyridine using the TD-DFT method[23] are consistent with the experimental values. In the frontier orbitals of both **3** and **5**·pyridine, the pyridine units are not involved at all, which excludes the fluorescence quenching by the orbital-interaction.

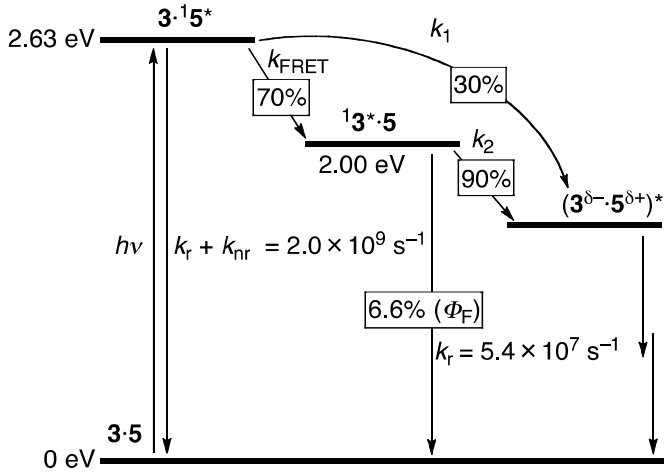

Figure 8. An energy diagram for FRET and sequential fluorescence quenching pathways of **3**·**5**. The energy values are relative to that of the ground state of **3**·**5**.

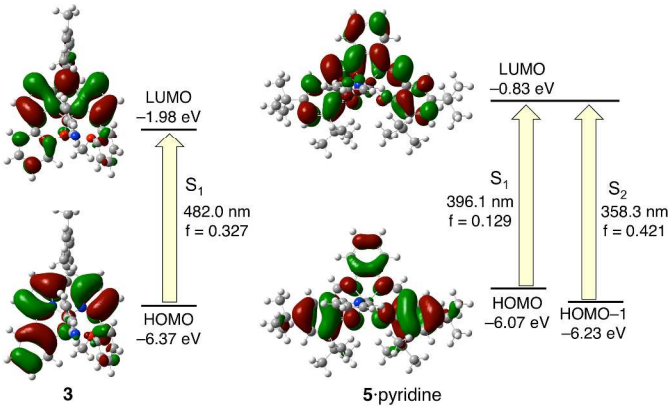

Figure 9. The Kohn–Sham frontier orbitals and vertical transition energies of **3** (left) and **5**·pyridine (right) calculated by TD-DFT method at the M06-2X/6-31G(d,p).

When excited at 420 nm, Φ_{flu} of **3**·**5** was 4.8%, which is smaller than that observed when excited at 600 nm (6.6%). If the energy transfer in **3**·^{1}**5*** is much faster than the direct decay ($k_r + k_{nr}$) as described in the case of **4**·^{1}**5***,[24] the efficiency of the quenching path from **3**·^{1}**5*** (k_1) can be 27% (Figure 8) based on the quantum yields. The efficiency (30%) estimated from the excitation spectrum is almost the same as that estimated from quantum yields (Figure S12). The quenching efficiency from ^{1}**3***·**5** (k_2) was determined to be 88% based on the assumption that k_r and k_{nr} values of ^{1}**3***·**5** are identical to those of ^{1}**3***. These results suggest the efficient fluorescence quenching in **3**·**5**. The distance between the BODIPY core and the **5** unit in **3**·**5** linked by a 3-pyridyl group should be shorter than that of **4**·**5** by a 4-pyridyl group. The closely positioned BODIPY and **5** can be expected to make a fluorescence-quenching pathway via exciplex formation possible.

Conclusions

Dipyrrin–boronic acid dyad **2** and dipyrrin–boronic acid–Zn complex triads **3**·**5** and **4**·**5**, which possess energy donor units, were synthesized. The dyad **2** and triad **4**·**5** collected short-wavelength light at the donor units, and then underwent quantitative FRET to the fluorophore *Ar*,*O*-BODIPY unit. As a result, the dyad **2** and triad **4**·**5** emitted fluorescence by collecting light across a wide visible region. Interestingly, the fluorescence quenching process in the excited state of the triad **3**·**5** took place following the energy transfer event. Thus, an appropriate positioning of the energy donor and acceptor is necessary to construct a highly efficient FRET system. Our present results represent a facile FRET system across a wide range of the visible region, which is expected to be applicable to a light-harvesting system as seen in nature.

Acknowledgements

This research was financially supported by Grants-in-Aid for Scientific Research (Innovative Area: Stimuli-responsive Chemical Species) from the Ministry of Education, Culture, Sports, Science, and Technology of Japan.

Notes and references

[a] Graduate School of Pure and Applied Sciences & Tsukuba Research Center for Interdisciplinary Materials Science, University of Tsukuba, 1-1-1 Tennodai, Tsukuba, Ibaraki 305-8571, Japan.
[b] Graduate School of Engineering, Osaka Prefecture University, 1-1 Gakuen-cho, Sakai, Osaka 599-8531, Japan.

† Electronic Supplementary Information (ESI) available: NMR and MS charts and computational results. See DOI: 10.1039/b000000x/

1 D. E. Metzler, in *Biochemistry: The Chemical Reactions of Living Cells, 2nd Ed.*, Academic Press: San Diego, 2003, pp 1298–1324.
2 J. Yang, M. Yoon, H. Yoo, P. Kim, and D. Kim, *Chem. Soc. Rev.* 2012, **41**, 4808–4826.
3 (a) A. Loudet and K. Burgess, *Chem. Rev.* 2007, **107**, 4891–4932; (b) T. E. Wood and A. Thompson, *Chem. Rev.* 2007, **107**, 1831–1861.
4 (a) F. R. Li, S. I. Yang, Y. Z. Ciringh, J. Seth, C. H. Martin, D. L. Singh, D. H. Kim, R. R. Birge, D. F. Bocian, D. Holten, and J. S. Lindsey, *J. Am. Chem. Soc.* 1998, **120**, 10001–10017; (b) Z. Kostereli, T. Ozdemir, O. Buyukcakir, and E. U. Akkaya, *Org. Lett.* 2012, **14**, 3636–3639.
5 (a) C. Goze, G. Ulrich, L. Charbonnière, M. Cesario, T. Prangé, and R. Ziessel, *Chem. Eur. J.* 2003, **9**, 3748–3755; (b) Y. Gabe, Y. Urano, K. Kikuchi, H. Kojima, and T. Nagano, *J. Am. Chem. Soc.* 2004, **126**, 3357–3367; (c) A. Coskun, and E. U. Akkaya, *J. Am. Chem. Soc.* 2005, **127**, 10464–10465.
6 (a) T. Kobayashi, T. Komatsu, M. Kamiya, C. Campos, M. González-Gaitán, T. Terai, K. Hanaoka, T. Nagano, and Y. Urano, *J. Am. Chem. Soc.* 2012, **134**, 11153–11160; (b) N. Ieda, Y. Hotta, N. Miyata, K. Kimura, and H. Nakagawa, *J. Am. Chem. Soc.* 2014, **136**, 7085–7091.
7 (a) S. P. Singh and T. Gayathri, *Eur. J. Org. Chem.* 2014, 4689–4707; (b) S. Kolemen, O. A. Bozdemir, Y. Cakmak, G. Barin, S. Erten-Ela, M. Marszalek, J.-H. Yum, S. M. Zakeeruddin, M. K.

Nazeeruddin, M. Grätzel, and E. U. Akkaya, *Chem. Sci.* 2011, **2**, 949–954; (c) Y. Kubo, D. Eguchi, A. Matsumoto, R. Nishiyabu, H. Yakushiji, K. Shigaki, and M. Kaneko, *J. Mater. Chem. A* 2014, **2**, 5204–5211.

8 (a) G. Ulrich, C. Goze, M. Guardigli, A. Roda, and R. Ziessel, *Angew. Chem., Int. Ed.* 2005, **44**, 3694–3698; (b) C. Goze, G. Ulrich, L. J. Mallon, B. D. Allen, A. Harriman, and R. Ziessel, *J. Am. Chem. Soc.* 2006, **128**, 10231–10239; (c) A. Harriman, G. Izzet, and R. Ziessel, *J. Am. Chem. Soc.* 2006, **128**, 10868–10875.

9 M. Tsuchiya, R. Sakamoto, S. Kusaka, Y. Kitagawa, M. Okumura, and H. Nishihara, *Chem. Commun.* 2014, **50**, 5881–5883.

10 C. Ikeda, T. Maruyama, and T. Nabeshima, *Tetrahedron Lett.* 2009, **50**, 3349–3351.

11 (a) D. G. Hall (Ed.), in *Boronic Acids*, WILEY-VCH, Weinheim, 2005, pp 1–100; (b) K. Tsukagoshi and S. Shinkai, *J. Org. Chem.* 1991, **56**, 4089–4091. (c) G. Deng, T. D. James, and S. Shinkai, *J. Am. Chem. Soc.* 1994, **116**, 4567–4572. (d) N. Iwasawa and H. Takahagi, *J. Am. Chem. Soc.* 2007, **129**, 7754–7755.

12 (a) N. Sakamoto, C. Ikeda, M. Yamamura, and T. Nabeshima, *J. Am. Chem. Soc.* **2011**, *133*, 4726–4729; (b) M. Yamamura, H. Takizawa, N. Sakamoto, and T. Nabeshima, *Tetrahedron Lett.* 2013, **54**, 7049–7052; (c) M. Yamamura, M. Albrecht, M. Albrecht, Y. Nishimura, T. Arai, and T. Nabeshima, *Inorg. Chem.* 2014, **53**, 1355–1360.

13 C. Ikeda, S. Ueda, and T. Nabeshima, *Chem. Commun.* 2009, 2544–2546.

14 N. Amann, E. Pandurski, T. Fiebig, and H.-A. Wagenknecht, *Angew. Chem. Int. Ed.* 2002, **41**, 2978–2980.

15 D. Cai, R. D. Larsen, and P. J. Reider, *Tetrahedron Lett.* 2002, **43**, 4285–4287.

16 M. E. Germain, T. R. Vargo, P. G. Khalifah, and M. J. Knapp, *Inorg. Chem.* 2007, **46**, 4422–4429.

17 (a) K. Suzuki, A. Kobayashi, S. Kaneko, K. Takehira, T. Yoshihara, H. Ishida, Y. Shiina, S. Oishi, and S. Tobita, *Phys. Chem. Chem. Phys.* 2009, **11**, 9850–9860; (b) H. Ishida, S. Tobita, Y. Hasegawa, R. Katoh, and K. Nozaki, *Coord. Chem. Rev.* 2010, **254**, 2449–2458.

18 M. J. Frisch, et al. *Gaussian 09, Revision A.02*, Gaussian, Inc., Wallingford CT, 2009.

19 Y. Zhao and D. G. Truhlar, *Theor. Chem. Acc.* 2008, **120**, 215–241.

20 (a) A. W. Kleij, *Eur. J. Inorg. Chem.* 2009, 193–205. (b) A. W. Kleij, *Chem. Eur. J.* 2008, **14**, 10520–10529. (c) S. J. Wezenberg and A. W. Kleij, *Angew. Chem., Int. Ed.* 2008, **47**, 2354–2364. (d) S. Akine and T. Nabeshima, *Dalton Trans*. 2009, 10395–10408.

21 As the quenching process, photoinduced electron transfer, PeT, which is often considered as fluorescence quenching, is excluded. Free energy change (ΔG_{PeT}) in PeT from **5** to **3*** can be determined from the Rehm–Weller equation (Eq 1). See: D. Rehm and A. Weller, *Isr. J. Chem.* 1970, **8**, 259–271.

$$\Delta G_{PeT} = E_{ox} - E_{red} - E^{0-0} + w \quad \text{(Eq 1)}$$

The calculated ($E_{ox} - E_{red} - E^{0-0}$) value is so small (–0.24 eV) that ΔG_{PeT} value should be positive in nonpolar solvent, *n*-hexane.

22 Although transient absorption measurements were performed to gain insight into an intermediate during fluorescence quenching, any absorption assignable to exciplex was not observed. In the case of **3**·**5**, long-lived absorption bands were observed at 460 and 660 nm at the lifetime of 70~80 μs (Figures S17 and S18). The observed species might be some excited triplet species generated via intersystem crossing of exciplex. The quenching pathway via intersystem crossing is excluded because the energy level of ^{3}**5*** (2.07 eV), which is estimated by phosphorescence (Figure S15), is higher than that of ^{1}**3*** (2.00 eV).

23 There is a simple linear correction between the M06-2X excitation energy of BODIPYs and the experimental value, (0.908 × E_{calc} −0.141) eV. The correlated excitation energy of **3**, 565 nm, well matches the experimental value, 595 nm. See: S. Chibani, B. Le Guennic, A. Charaf-Eddin, A. D. Laurenta, and D. Jacquemin, *Chem. Sci.* 2013, **4**, 1950–1963.

24 FRET process is effective even when the distance between donor and acceptor is relatively long (1.0~10 nm). The distances between donor and acceptor in the model structures of **3**·**5** and **4**·**5** are close enough to permit FRET. See: Figures S20 and S21 in the Supporting Information.